La-promoted Ni/γ-Al₂O₃ catalyst for autothermal reforming of methane

Mahmood Alam Khan and Seong Ihl Woo†

Department of Chemical and Biomolecular Engineering, Korea Advanced Institute of Science and Technology (KAIST),
373-1, Guseong-dong, Yeuseong-gu, Daejeon 305-701, Korea
(*Received 5 September 2013 • accepted 5 February 2014*)

Abstract−Autothermal reforming (ATR) of methane over the synthesized catalysts of 10Ni-2La/γ-Al₂O₃, 10Ni-2Ce/γ-Al₂O₃, 10Ni-2Co/γ-Al₂O₃ was investigated in the temperature range of 600-800 °C for the hydrogen production. The sequence of 2 wt% metal loading on nickel alumina support in relation to their catalytic performance was observed as La>Ce>Co. The excellent activity and selectivity of 10Ni-2La/γ-Al₂O₃ was superior to other catalysts owing to little carbon deposition (~2.23 mg coke/gcat·h), high surface area and good dispersion and stability in the alumina support. The reforming of methane was inferred to be initiated by the decomposition of hydrocarbon at the inlet zone, preceded by the reforming reactions in the catalyst bed. Our result shows that it can be possible to achieve the H_2/CO ratio optimal to the GTL processes by controlling the O_2/CH_4 ratio of the feed inlet. The addition of oxygen to the feed inlet enhanced conversion efficiency substantially; probably, it favors the re-oxidation of carbonaceous residues formed over the catalyst surfaces, avoiding the catalyst deactivation and hence promoting catalyst stability.

Keywords: GTL Process, Synthesis Gas, 10Ni-2La/γ-Al₂O₃, Catalysis, Hot Spot, ATR

INTRODUCTION

Hydrogen gas is perceived as a potentially important energy carrier fuel for a clean and sustainable future [1,2]. It has been estimated that the world's hydrogen and fuel cell market will grow 16 billion dollars by the year 2017 [3]. Meanwhile, the staggering demand for chemicals derived from the syngas synthesis has led to the development of many renewed processes such as hydrogen based fuel cell engines which are expected to lower emissions of harmful gases such as SOx, NOx and CO. At present, the most common source of syngas is hydrocarbons, particularly natural gas (CH_4) [4]. This natural gas can be easily extracted from an estimated recoverable world reserve of 8×10^{15} ft³ [5]. The most common technology widely used for the production of the syngas is catalytic methane reaction with steam SRM to produce a mixture of hydrogen, carbon monoxide and carbon dioxide, although ongoing research has proposed some alternative processes [6].

Several reports have addressed the development of specific catalysts for the methane oxy-steam reforming processes [7,8], and the catalysts based on Ni supported Mg-AlO spinels [9] are already in use for the steam reforming reactions. To date, various families of catalysts investigated in commerce are composed of NiO supported on ceramic materials (α-AlO, MgO, MgMAlO spinel, ZrO) [10]. The catalyst composition presents an averaged content of NiO equal to 15%, although this value could reach extremes of 7 wt% to 79 wt% and still offer an appreciable amount of catalytic activities and good stabilities with lower prices.

Partial oxidation is an exothermic reaction with abundant heat production, whereas steam reforming is an endothermic reaction. Hence, partial oxidation could easily start up on ignition even without a catalyst, but conversion efficiencies are low as the released heat is wasted. Whereas, the disadvantage of steam reforming is in the large extent of its heating for the reactor and steam generator. But autothermal reforming is the combination of the reforming and partial oxidation adiabatically, where steam reforming of hydrocarbons is carried out in the presence of oxygen to produce suitable H_2/CO ratio without any external energy consumption. It has low-energy requirements due to the opposite contribution of the exothermic methane oxidation and endothermic steam reforming reactions. On the other hand, the efficiencies could be enhanced when steam reforming of hydrocarbons is combined, which can improve the reactor temperature control and reduce the formation of hot spots, avoiding catalyst deactivation by sintering or carbon deposition. Moreover, ATR allows the production of syngas with a wider range of H_2/CO ratio by manipulating the relative concentrations of H_2O and O_2 in the feed inlet as the H_2/CO ratio of ~2 is necessary to GTL plants [11-18]. In addition, a fuel processor based on autothermal reforming of methane could provide a low cost and compact system, with fast start-up and capability to follow load variations adequately, an essential criterion for fuel cell electric vehicles. Exothermic, endothermic, and thermo-neutral condition can be selected by choosing an appropriate ratio of hydrocarbon: oxygen: steam [19,20]. All these advantages indicate that ATR should be the technology of choice for large-scale GTL plants, and this process is relatively compact and has greater potential for economic scale up [21]. It can be described as a catalytic autothermal reforming process and can be represented as

$$CH_4+xO_2+yH_2O=aCO+bCO_2+cH_2O$$
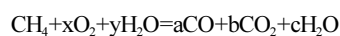
where x is the $O_2=(O_2/CH_{4\,feed})/X$, y is the $H_2O_{reacted}/(CO+CO_2)_{reformate}$, a is the $=(CO/CH_{4\,feed})/X$, b is the $(CO_2/CH_{4\,feed})/X$, c is the H_2 ($H_2/CH_{4\,feed}$)/X, and X is the CH_4 conversion=$(CO+CO_2)_{reformate}/(CO+CO_2+CH_4)_{reformate}$. Here the assumption is based on all of the O_2 being

†To whom correspondence should be addressed.
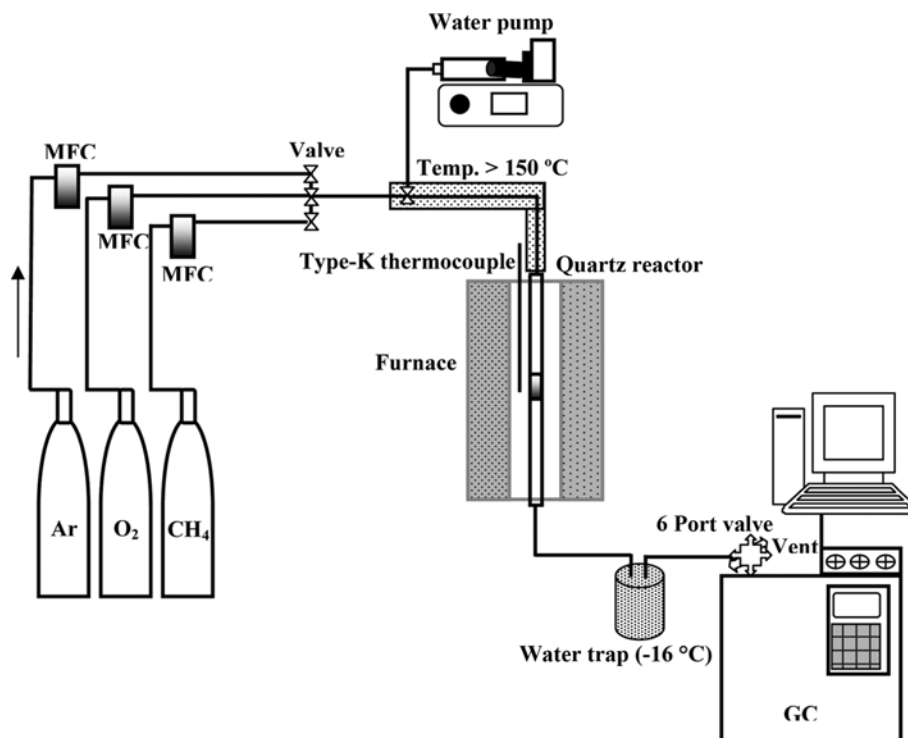E-mail: siwoo@kaist.ac.kr

Fig. 1. Schematic diagram of the experiment set-up for the autothermal reforming (ATR) of methane.

consumed in autothermal reaction with no deposition of any coke. The heat of reaction (ΔH_R) depends on the temperature and on the fractions of oxygen and water in feed inlet. ATR technology normally operates at large-scale under the conditions, where reaction temperatures are varied frequently at startup and shutdown of the operation. Thus, a robust and coke-resistant catalyst must be in need which can withstand multiple cycles and also possesses tolerance under unusual transient conditions without deterioration.

Previous studies have shown that the addition of promoters such as Ce and La to ZrO_2 supports results in improved catalytic performance for the dry reforming reactions [22]. Besides the theoretical aspects involved in the development of the ATR process, a suitable and active catalyst needs to be available for commercialization. In the present study, we investigated the comparative behavior of three catalysts (10Ni-2La/γ-Al₂O₃, 10Ni-2Ce/γ-Al₂O₃, 10Ni-2Co/γ-Al₂O₃) in autothermal reforming of methane with the variation of feed stream ratio of CH_4/O_2 to determine the behavior of supported metal catalysts in the ATR process. We aimed to develop an alternative, economical and robust autothermal reforming catalysts which would have high resistivity of coke formation without utilizing the doping of precious metals (Pt, Ru, Rh).

EXPERIMENTAL SECTION

The catalyst 10%Ni-2%La/γ-Al₂O₃ support was prepared as follows. First, 10 wt% of Ni was weighted using precursor $Ni(NO_3)_2$ (Aldrich) in distilled water of 50 ml in a beaker; then 2 wt% of La using precursor $La(NO_3)_2$ (Aldrich) was added in it and magnetically stirred for 60 min; then the 3 gm of γ-Al₂O₃ was added slowly with the continued stirring for 2 h. After that, the distilled water was removed from the slurry by using a rotary pump drying. The sample

was further dried at 80 °C in an oven for 4 h and then calcined at 550 °C for 2 h in a tubular reactor in the presence of air flow. The prepared catalyst was denoted as 10Ni-2La/γ-Al₂O₃. Similar method was applied for the 10Ni-2Ce/γ-Al₂O₃, 10Ni-2Co/γ-Al₂O₃, and 10Ni/γ-Al₂O₃, where metal precursors were used in the form of nitrate salts.

The schematic reaction setup is shown in Fig. 1. Prior to the actual reaction the catalyst was reduced in the 20% H_2 flow for 30 min at 500 °C. The reaction was carried out in a fixed-bed flow quartz reactor with total length of 39 cm, 6 mm of outer diameter and 4 mm of inner diameter (the bed height is 5-6 mm), loaded with 0.25 g catalyst under atmospheric pressure. The catalyst bed was supported by quartz wool. The total feed flow was maintained at 200 ml/min with GSV of 4,500 h^{-1} flowing. A water pump was used to control the flow of steam in the reactor. The feed ratio of the gases is depicted in Table 1. An activity test was performed at different temperatures, ranging from 600 °C to 800 °C in ramps of 50 °C which was kept at 60 min. The loss in catalyst activity at 750 °C was monitored up to 30 h on feed gas stream. For the comparison blank experiments were also carried out at 750 and 800 °C but conversion was found negligible. The reaction product was analyzed by on-line gas chromatograph (HP-6890) equipped with two columns and thermal con-

Table 1. Details of methane gas flow rates for the activity measurements on tested parameters (cm³/min)

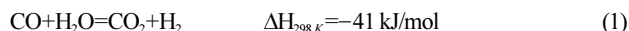| O_2/CH_4	H_2O/CH_4	O_2	CH_4	H_2O	Ar	Total feed
0.25	1.0	10	40	40	150	200
0.5	1.0	20	40	40	100	200
1.0	1.0	40	40	40	80	200
1.5	1.0	60	40	40	60	200

ductivity detector (TCD).

The X-ray diffraction patterns (XRD) were taken with Rigaku (D/MAX 2500, Japan) equipped with Cu Kα radiation ($\lambda \kappa$=0.154 nm). The amount of coke formed over catalyst after deactivation at 750 °C was examined by thermogravimetric analysis (TGA) using (TG209F3). The sample was pretreated at 150 °C under flowing of oxygen at heating rate of 10 °C/min to 800 °C in flow of 20% O_2/Ar. Transmission electron microscope (TEM) analysis was measured by JEOL 1200 microscope and the images were taken at 120 KeV with magnification of 100 to 500 KeV. Brunauer-Emmett-Teller (BET) surface area was analyzed by Micromeritics ASAP 2100.

RESULTS AND DISCUSSION

1. Temperature Effects

Autothermal reforming reaction of methane over the synthesized catalysts and their comparative activities is depicted in the Fig. 2(a) and (b) with a constant feed ratio of H_2O/CH_4 of 1.0 and O_2/CH_4 of 0.5 in respect to the CH_4 conversions, and the ratios of H_2/CO products, respectively. The maximum CH_4 conversion efficiency up to 91% was achieved with the 10Ni-2La/γ-Al_2O_3 catalysts at 750-
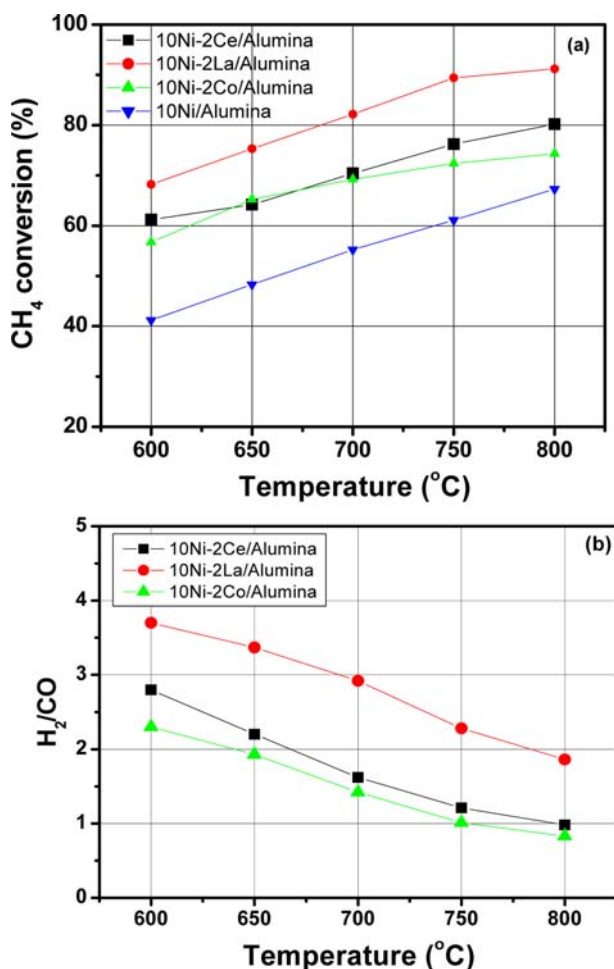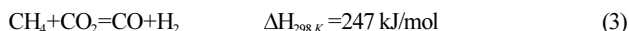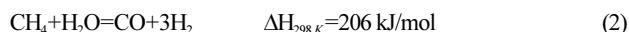

Fig. 2. The catalytic activities from the synthesized catalysts in relation to CH_4 conversion efficiency as a function of temperature (a) catalysts for autothermal reforming of methane and (b) with product ratio of H_2/CO generation.

800 °C; however, 80% and 74% conversion efficiencies were observed with the 10Ni-2Ce/γ-Al_2O_3, 10Ni-2Co/γ-Al_2O_3 catalysts, respectively. Bare 10Ni/γ-Al_2O_3 shows lower activity than the synthesized catalysts. The H_2/CO generation ratio was also higher in the case of 10Ni-2La/γ-Al_2O_3 which was about 3.7 (Fig. 2(b)), especially at low temperature regime. The high H_2/CO ratio (3.7) at 600 and 650 °C with the catalyst 10Ni-2La/γ-Al_2O_3 suggests that the water-gas shift (WGS) reaction may occur with the reforming of methane at lower temperatures, as already has been reported [23, 24]. However, with the increase of reaction temperature the H_2/CO ratio decreases, which is also consistent with the fact that WGS is thermodynamically unfavorable at higher temperatures:

$$CO+H_2O=CO_2+H_2 \qquad \Delta H_{298\,K}=-41 \text{ kJ/mol} \qquad (1)$$

At higher temperature (750 °C) H_2/CO ratio was observed ~2.1 for 10Ni-2La/γ-Al_2O_3, 1.6 for 10Ni-2Ce/γ-Al_2O_3 and 1.4 for 10Ni-2Co/γ-Al_2O_3 indicating that the reverse of WGS reaction may takes place simultaneously with the autothermal reforming of methane as depicted below:

$$CH_4+H_2O=CO+3H_2 \qquad \Delta H_{298\,K}=206 \text{ kJ/mol} \qquad (2)$$

$$CH_4+CO_2=CO+H_2 \qquad \Delta H_{298\,K}=247 \text{ kJ/mol} \qquad (3)$$

In the literature, a two-step mechanism for the partial oxidation of methane has been reported. In the first step partial oxidation of methane takes place producing CO_2 and H_2O, and in the second step synthesis gas is produced via steam reforming reactions of unreacted methane [25-27]. This indirect mechanism can also give an evidence for high activity autothermal reforming of methane as can be seen from the Fig. 2 for 10Ni-2La/γ-Al_2O_3 catalyst. With the decreasing temperature, water conversion is lower than methane conversion owing to the combustion of methane which produces CO_2 and H_2O. According to the reported literature, the reaction mechanism can be related to the change in the Ni valence state during the partial oxidation of methane. The transformation of reaction from complete oxidation of methane to partial oxidation was associated with methane reduction of NiO to Ni^0 [25] by hydrogen from water during reforming reaction. Additionally, the small amount of La doping promoted catalyst surface efficiently and increased methane autothermal reforming by superior selectivity and good bindings with supports, reduced the coke formation, may bind well with nickel, and hence helped to increase in its overall activity, while Ce and Co dopings were less effective, possibly bigger size of doped metal catalyst as shown in TEM image (Fig. 8).

2. Effect of Time on Feed Stream

Fig. 3 shows inlet feed stream effects on the time duration for 30 h reaction analysis at 750 °C with constant feed ratio of H_2O/CH_4 of 1.0, and O_2/CH_4 ratio of 0.5. The catalysts showed a different initial reaction activities and also different deactivation rates clearly. The catalyst 10Ni-2La/γ-Al_2O_3 showed the highest initial reaction activities (~92%) and also its deactivation rate was lower (76%) with mean deactivation rate of 0.53%/h on the stream of 30 h testing. However, in the case of 10Ni-2Ce/γ-Al_2O_3 catalysts initial activity was lower, and deactivation rate was also fast from 82% to 48% with the mean deactivation rate of 1.13%/h in the 30 h reaction regimen. However, in case of 10Ni-2Co/γ-Al_2O_3 the activity was 74% to 34% with mean deactivation rate of 1.33%/h in 30h
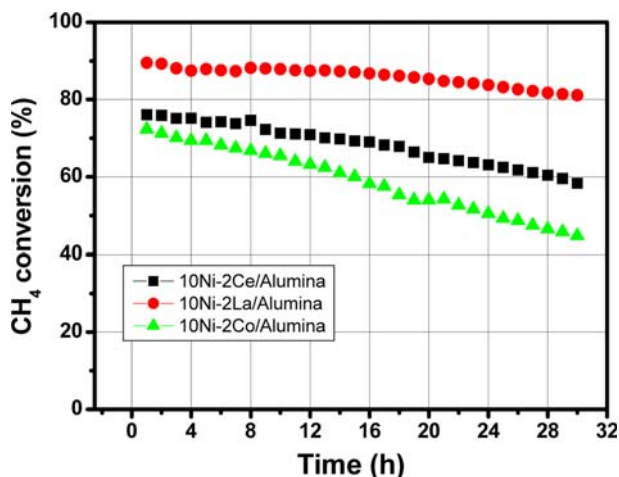
Fig. 3. The deactivation test in autothermal reforming in respect to CH$_4$ conversion with relation to time on inlet feed stream at 750 °C.
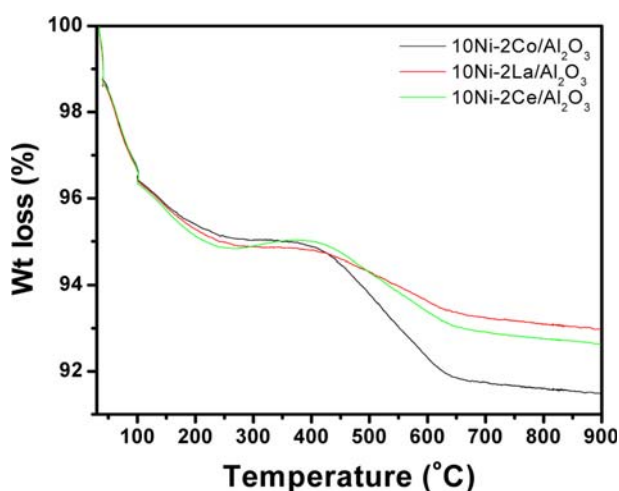

Fig. 4. Thermogravimetric analysis of the prepared catalysts after their deactivation test at 750 °C for 30 h in 20% O$_2$/Ar at 20 °C/min ramp.

reaction stream. The deactivation may be related to the deposition of coke formation over the active sites of the catalysts, and the amount of the coke on these catalysts was analyzed by thermogravimetric analysis carried out in oxygen atmosphere (20% O$_2$+80% Ar) as depicted in the Fig. 4. It was observed that the stability of the 10Ni-2La/γ-Al$_2$O$_3$ was associated with the observation of little coke formation during the reaction (~2.23 mg coke/gcat·h). On the other hand, coke formation in 10Ni-2Ce/γ-Al$_2$O$_3$ and 10Ni-2Co/γ-Al$_2$O$_3$ indicated greater amount of carbon deposition during 30h on feed gas stream (2.4 and 3.1 mg coke/gcat.h, respectively). The deposition of inactive coke during methane reforming reaction can originate from either methane decomposition as (4)

$$CH_4 = C + 2H_2 \qquad \Delta H_{298\,K} = 75 \text{ kJ/mol} \qquad (4)$$
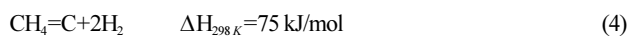
or, CO disproportionation (Boudouard) reaction (5), which are thermodynamically favorable below 900 °C.

$$2CO = C + CO_2 \qquad \Delta H_{298\,K} = -172 \text{ kJ/mol} \qquad (5)$$
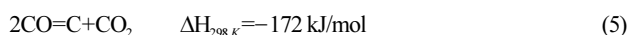
Thermodynamic calculations showed that the extent of carbon deposition during reforming decreases at higher reaction temperatures, which is in agreement with several similar experimental works [28, 29]. These results suggested that the CO disproportionation is the main contributor of carbon deposition because it is exothermic and the equilibrium constant decreases with increasing temperatures. The high stability of 10Ni-2La/γ-Al$_2$O$_3$ catalyst is closely related to its resist to coke formation, which can be attributed to high surface area (BET analysis), better Ni-La interaction with alumina support interface and high stabilization of catalysts. The number of interfacial sites is higher on this catalyst compared to others because the particle size of La is smaller (TEM analysis Fig. 8(a)) than Ce and Co metals; therefore, it is conjectured that the La particles are better dispersed in the support. As mentioned earlier, in the ATR reactor at higher temperature, first an exothermic reaction occurs in the presence of oxygen; where methane combustion takes place, it oxidizes Ni to NiO and coking takes place and in the second step of steam reforming, which is endothermic, excited by the energy gain of exothermic reaction, a breakdown of H$_2$O where hydrogen generated reduced the NiO to Ni. However due to complexity of reaction it is still not very clear how exactly the processes take place on the metal (Ni) and promoter (La) catalysts. It is speculated that not only resistance to coke formation but also predicted strong La-Ni-support interaction driving force may exist and La in less amount leads it to efficient catalytic effect.

3. The Effect of O$_2$/CH$_4$ Feed Ratio on Catalysts

Fig. 5 represents the CH$_4$ conversion efficiency at constant H$_2$O/CH$_4$ ratio of 1.0, O$_2$/CH$_4$ ratio of 0.5 at 750 °C with the function of time, and with variation of O$_2$/CH$_4$ feed ratio to 0.5, 1.0 and 1.5, respectively, on feed stream with 10Ni-2La/γ-Al$_2$O$_3$ catalyst. The increase in the O$_2$/CH$_4$ inlet feed ratio not merely increases the CH$_4$ conversions but also decreases the catalyst deactivations, probably due to coke formation. When the O$_2$/CH$_4$ ratio was 1.0 there was slight activation of the catalyst with passing time on stream, and when the ratio increased to 1.5 the CH$_4$ conversion was almost 98% throughout the reaction duration of 30 h reaction. Increase in the
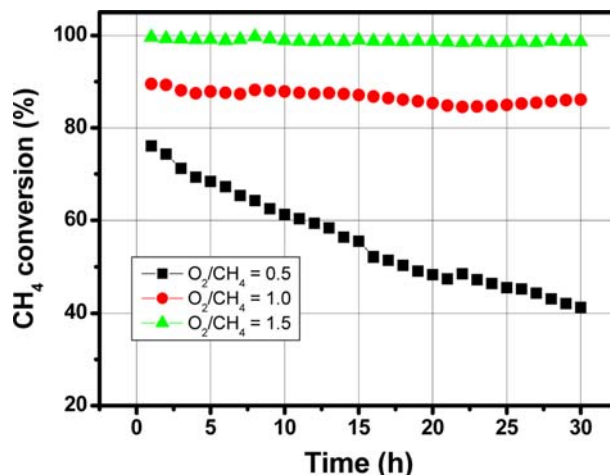

Fig. 5. The methane conversion observed in respect to the function of time on feed stream, at 750 °C with the variation of the O$_2$/CH$_4$ inlet feed ratio for the best synthesized 10Ni-2La/γ-Al$_2$O$_3$ catalyst.
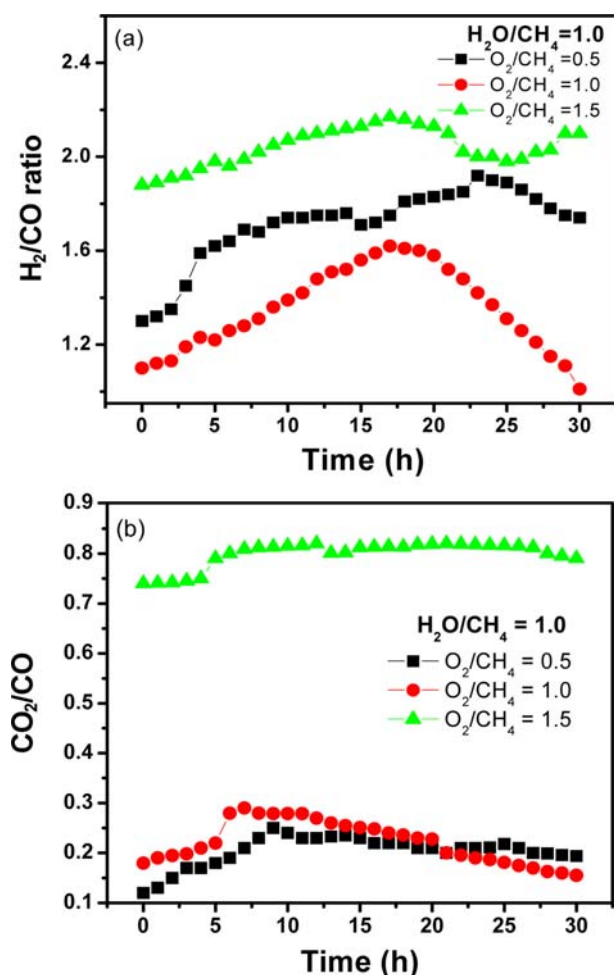
Fig. 6. Catalytic selectivity in respect to time on feed stream at 750 °C in terms of (a) H$_2$/CO ratio and (b) CO$_2$/CO product ratios for the best 10Ni-2La/γAl$_2$O$_3$ catalyst.

Fig. 7. XRD diffraction pattern of the synthesized catalyst 10Ni-2La/γ-Al$_2$O$_3$.

oxygen ratio in the catalytic feed has been already observed by several authors during the steam reforming [24], CO$_2$ reforming of methane [30]. The excess of O$_2$ probably favors the re-oxidation of carbonaceous residues formed over the catalyst surfaces, avoiding catalyst deactivation. The increase in the oxygen ratio in CH$_4$ conversion can be related to two distinct effects: one being the fast combustion of methane with the oxygen in the feed, another being increase in the reforming reaction rate due to increase in temperature caused by exothermic effects of the reaction. The comparison of the catalyst selectivity's at 750 °C with different O$_2$/CH$_4$ feed ratio is displayed in Fig. 6(a) and (b) in terms if H$_2$/CO and CO$_2$/CO ratio, respectively. The H$_2$/CO ratio was observed as low as (1.61) when the O$_2$/CH$_4$=1.0; this ratio reached to 1.89 when O$_2$/CH$_4$=1.5. The CO$_2$/CO ratio is about 0.27 for O$_2$/CH$_4$<1.0 and 0.8 for O$_2$/CH$_4$= 1.5. The role of oxygen addition on the catalytic selectivity is fairly complicated due to the different contributions of reactions as shown in Eqs. (1) to (4). When O$_2$/CH$_4$ ratio was 1.0, then the CO$_2$/CO ratios had almost the same value, which indicates that the total combustion proceeds to the same extent, but the reforming reaction is enhanced by decreasing O$_2$/CH$_4$ ratio due to the higher relative availability of methane under these conditions. When the ratio O$_2$/CH$_4$ was 1.5, the H$_2$/CO ratio obtained was (~2), which has the opti-
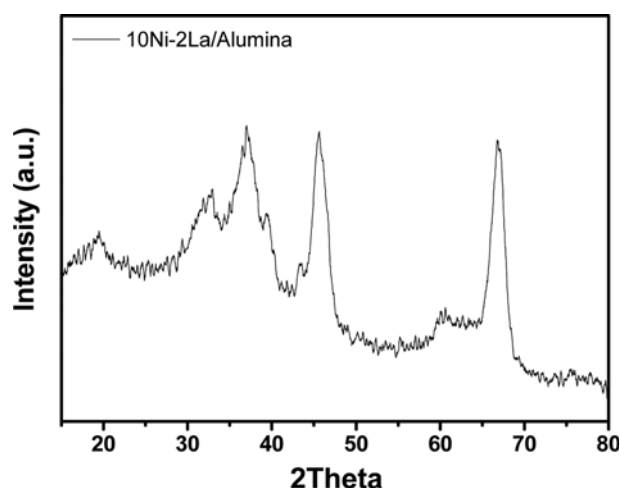
mum value for GTL processes; however, the H$_2$ and CO yields were lower, with relative to higher formation of CO$_2$ and H$_2$O by methane combustion reactions. Fig. 7 shows that the XRD pattern of 10Ni-2La/γ-Al$_2$O$_3$ catalyst, which is dominated by alumina peaks, can be well indexed to γ-Al$_2$O$_3$ (JCPDS No.47-1308), the smaller peaks position at 43.49° indexed as Ni peak and peak at 19.59° signifies that trace peak of Al^{3+} is present there with the doped metals probably due to formation of aluminum coated composite. These composites may act as pinning centers sticking the heteroatoms to the aluminum surface, which provides a good structural stability of the composite material between the deposited particle and the surface of the host, making it a robust and efficient catalyst. Fig. 8(a), (b), (c) shows the TEM images of doped metal catalyst of the synthesized samples after the reduction in 20% H$_2$ in argon atmosphere. It was observed that metal particles of promoter in the 10Ni-2La/γ-Al$_2$O$_3$, 10Ni-2Ce/γ-Al$_2$O$_3$, 10Ni-2Co/γ-Al$_2$O$_3$ have particle length of 25 nm, 32.1 nm and 48 nm, respectively. Fig 8(d) shows the image after the reaction was carried out at 750 °C for 30 h for the best catalyst (10Ni-2La/γ-Al$_2$O$_3$) where a small increase of particle size of 6 nm was observed along with the visible amount of coke. BET surface area was measured and found to be 27, 21 and 17 m^2/g of the synthesized catalyst after the reduction. BET surface area of the best catalyst (10Ni-2La/γ-Al$_2$O$_3$) after the reaction of 30 h at 750 °C was also measured and found to be around 15 m^2/g, possibly due to deposition of some amount of coke, which is consistent with the TGA and TEM analysis results.

CONCLUSIONS

The presence of 2 wt% La as a promoter in nickel and γ-Alumina support (10Ni-2La/γ-Al$_2$O$_3$) catalyst has been tested along with the 10Ni-2Ce/γ-Al$_2$O$_3$, 10Ni-2Co/γ-Al$_2$O$_3$ series and was found to be decisively superior and a promising candidate in GTL technology for the autothermal reforming (ATR) of methane with the least decativity of 0.53%/h at the feed stream of 200 ml/min flow at continuous monitoring of 30 h at 750 °C. The composition profile was best when the stoichiometric feed ratio of H$_2$O/CH$_4$ of 1.0 and O$_2$/CH$_4$ feed was 0.5. The higher stability of the catalyst was attributed to
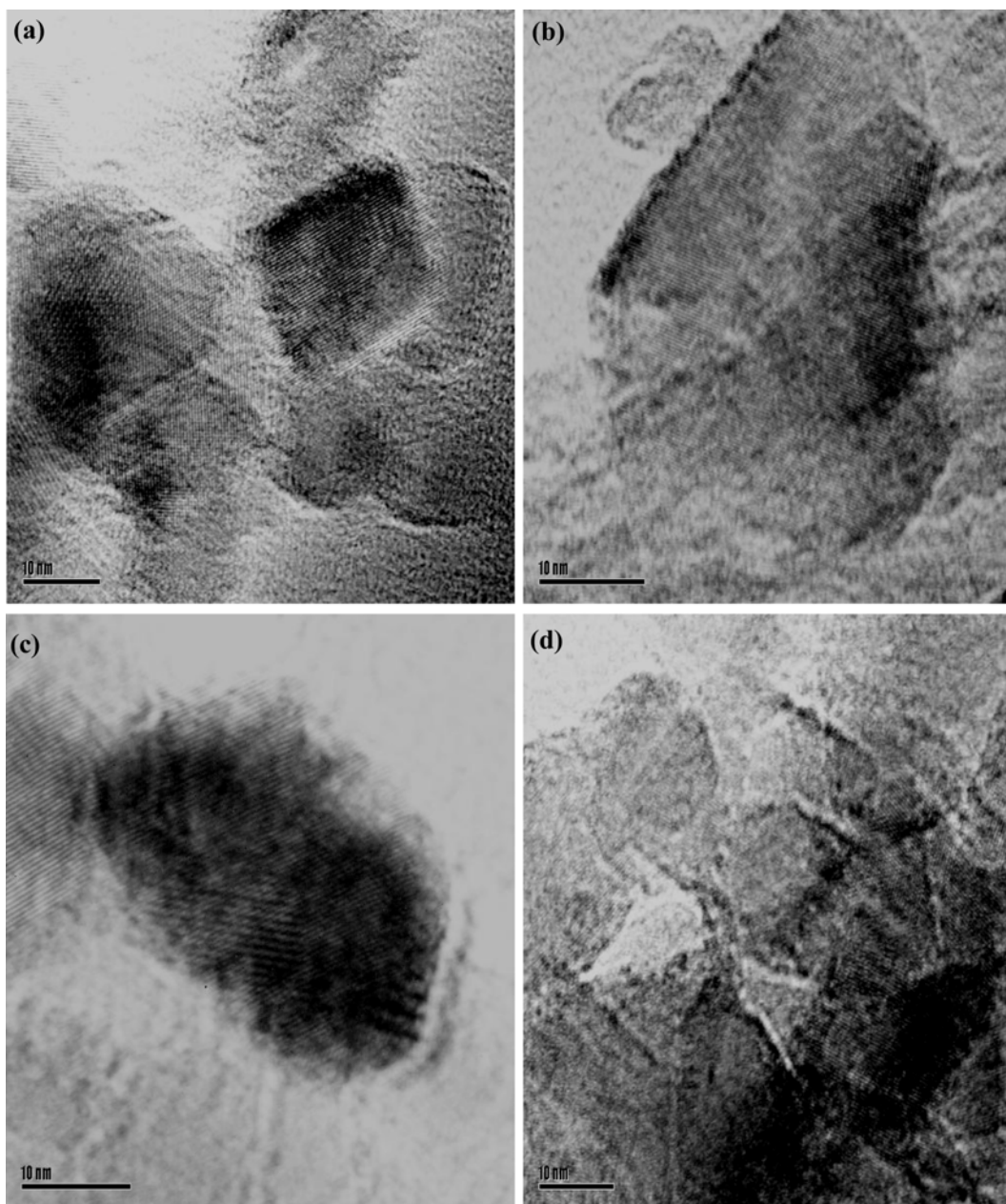
Fig. 8. TEM image of the metal supported catalyst after hydrogen reduction at 500 °C for 30 min (a) 10Ni-2La/γ-Al₂O₃ (b)10Ni-2Ce/γ-Al₂O₃ (c) 10Ni-2Co/γ-Al₂O₃ (d) La particle in 10Ni-2La/γ-Al₂O₃ after reaction at 750 °C for 30 h.

its resistance to coking and La-Ni-support interaction. The presence of 2 wt% La metal is promising in the GTL process as an economical candidate where no precious metal is utilized and can be a good alternate.

REFERENCES

1. V. A. Goltsov and T. N. Veziroglu, *Int. J. Hydrog. Energy*, **27**, 719 (2002).
2. J. Ohi, *Hydrogen energy futures: scenario planning by the U.S. DOE hydrogen technical advisory panel. In: Fourteenth world hydrogen energy conference*, Montreal, Canada, June 9-13 (2002).
3. *Hydrogen technology roadmap*, Australian Government, Department of Resources, Energy and Tourism (2008).
4. B. Jager, *Stud. Surf. Sci. Catal.*, **119**, 25 (1998).
5. M. Colitti, *Stud. Surf. Sci. Catal.*, **119**, 1 (1998).
6. S. Freni and S. Cavallaro, *Int. J. Hydrog. Energy*, **24**, 75 (1999).
7. V. R. Choudhary, B. S. Uphade and A. S. Mamman, *Appl. Catal. A*, **168**, 33 (1998).
8. V. R. Choudhary, A. M. Rajput and B. Prabhakar, *Angew. Chem. Int. Ed. Engl.*, **33**, 2104 (1994).
9. T. S. Christensen, *Hydrocarbon Process.*, **73**, 39 (1994).
10. J. R. Rostrup-Nielsen, Ed., *Catalysis, 5*, Springer, Berlin (1984).
11. P. D. F. Vernon, M. L. H. Green, A. K. Cheetham and A. T. Ash-

croft, *Catal. Lett.*, **6**, 181 (1990).

12. D. A. Hickman and L. D. Schmidt, *Science*, **259**, 343 (1993).

13. D. A. Hickman, E. A. Haupfear and L. D. Schmidt, *Catal. Lett.*, **17**, 223 (1993).

14. D. A. Hickman and L. D. Schmidt, *J. Catal.*, **138**, 267 (1992).

15. D. Dissanayake, M. P. Rosynek, K. C. C. J. Kharas and J. H. Lunsford, *J. Catal.*, **132**, 117 (1991).

16. P. M. Torniainen, X. Chu and L. D. Schmidt, *J. Catal.*, **146**, 1 (1994).

17. A. K. Bhattacharya, J. A. Breach, S. Chand, D. K. Ghorai, A. Hartridge, J. Keary and K. K. Mallick, *Appl. Catal., A*, **80**, 1 (1992).

18. H. Dong, Z. Shao, G. Xiong, J. Tong, S. Sheng and W. Yang, *Catal. Today*, **67**, 3 (2001).

19. S. Ahmed and M. Krumpelt, *Int. J. Hydrog. Energy*, **26**, 291 (2001).

20. V. R. Choudhary, B. S. Uphade and A. S. Mamman, *Micropor. Mesopor. Mater.*, **23**, 61 (1998).

21. A. T. Ashcroft, A. K. Cheetham, J. S. Foord, M. L. H. Green, C. P. Grey, A. J. Murreil and P. D. F. Vernon, *Nature*, **344**, 319 (1990).

22. S. M. S.-Williams, F. B. Noronha, G. Fendley and D. E. Resasco, *J. Catal.*, **194**, 240 (2000).

23. Z.-W. Liu, K.-W. Jun, H.-S. Roh and S.-E. Park, *J. Power Sources*, **111**, 283 (2002).

24. M. E. S. Hegarty, A. M. O'Connor and J. R. H. Ross, *Catal. Today*, **42**, 225 (1998).

25. D. Dissanayaki, M. P. Rosynek and J. H. Lunsford, *J. Phys. Chem.*, **97**, 3644 (1993).

26. E. P. J. Mallens, J. H. B. Hoebink and G. B. Martin, *Catal. Lett.*, **33**, 291 (1995).

27. F. van Looij, E. R. Stobbe and J. W. Geus, *Catal. Lett.*, **50**, 59 (1998).

28. M. C. J. Bradford and M. A. Vannice, *Catal. Rev. Sci., Eng.*, **41**, 1 (1999).

29. J. T. Richardson and S. A. Paripatyadar, *Appl. Catal.*, **61**, 293 (1990).

30. A. M. O'Connor and J. R. H. Ross, *Catal. Today*, **46**, 203 (1998).